Metamorphic Conditions of high-grade garnet-orthopyroxene-cordierite gneiss and garnet-cordierite gneiss from Mogok-Kyatpyin area of the middle segment of the Mogok metamorphic belt, central Myanmar

Ye Kyaw Thu[1], Khin San[2], Yin Kay Thwe Tun[3], Hay Mar Tun[4]

Abstract

The Cenozoic Mogok metamorphic belt lying at the western margin of the Shan-Thai Block forms a prominent part for understanding the continental evolution of Southeast Asia. The Mogok-Kyatpyin area occupies in the middle segment of the Mogok metamorphic belt and comprises high-grade gneiss associated with metacarbonate rock with the emplacement of granitoid rocks. The high-grade assemblages of gneiss samples from that area are characterized by Grt + Opx + Crd + Kfs + Pl + Bt + Qz + Ilm in HM22 sample, Grt + Crd + Kfs + Pl + Bt + Qz + Ilm in HM24 and with sillimanite inclusion BM01 samples, Grt + Sil + Kfs + Pl + Bt + Qz + Rt + Ilm in HM17 sample, and Grt + Kfs + Pl + Bt + Qz + Ilm in DT03 sample. In the KFMASH system for the metapelites of all bulk compositions, the average pressure and temperature ($P - T$) conditions of garnet-orthopyroxene-cordierite gneiss sample (HM22) and garnet-cordierite gneiss samples suggest 6.8 – 7 kbar/830 – 850 °C for the peak stage, respectively. The metamorphic conditions of the present study are consistent with the previously published estimations, and combining with other high-grade areas the present study suggest the widespread distribution of upper amphibolite to granulite facies metamorphic rocks in the middle segment of the Mogok belt. In addition, based on the formation of symplectitic cordierite grains, re-equilibration probably formed during the early stage of exhumation under upper-amphibolite or granulite facies conditions, and such extensive recrystallization combining with other reported areas likely occurred throughout the middle segment of the Mogok metamorphic belt at late Oligocene.

Key words: high-grade gneiss, Mogok-Kyatpyin area, metamorphic condition, granulite facies, re-equilibration

Introduction

The Mesozoic to Cenozoic tectonic evolution of Southeast Asia is characterized by the closure of the Tethyan oceans and subsequent collision of the Indian microcontinent with Eurasia (Metcalfe, 1994, 2013). Progressive convergence between these two continental plates resulted in the development of Cenozoic metamorphism and related magmatism in central Myanmar. The Cenozoic Mogok metamorphic belt, extending for about 1500 km, is exposed at the western margin of the Shan-Thai Block (Bunopas, 1982), and forms a prominent part for understanding the continental evolution of Southeast Asia. It consists of meta-igneous rocks and meta-sedimentary rocks with subduction-related granitoid intrusions.

Geochronological studies indicate that an assemblage of the Mogok high-grade metamorphic rocks formed during the Paleogene to early Neogene in association with the India–Eurasia continental collision (Bertrand et al., 1999; 2001; Barley et al., 2003; Searle et al., 2007; Maw Maw Win et al., 2016).

Peak metamorphic conditions appear to vary between different parts of the elongated belt, such as the amphibolite facies in the Kyanigan and Kyauske areas (e.g., Searle et al., 2007) and the granulite facies in the northern Mogok region (Yonemura et al., 2013) and the Sagaing ridge (Maw Maw Win et al., 2016). Ye Kyaw Thu et al. (2016) reported a paragneiss

[1]Assistant Lecturer, Department of Geology, Taungoo University
[2] Professor and Head, Department of Geology, Magway University
[3] Associate Professor, Department of Geology, Pakkoku University
[4] M.Sc Student, Department of Geology, Magway University

with a spinel + quartz assemblage coexisting with Ti-rich biotite (up to 6.9 wt% TiO_2) that formed under granulite facies conditions. These results imply that high-grade metamorphic rocks occur extensively in the western Shan-Thai Block.

However, mineralogical and petrological characteristics of the Mogok metamorphic rocks and their conditions have been poorly constrained. The present study combining with other reported areas attempts to deduce the metamorphic conditions of the garnet-orthopyroxene-cordierite gneiss and garnet-cordierite gneiss, which may provide understanding the metamorphism of the Mogok metamorphic belt.

Geological setting

The Mogok metamorphic belt occurs along the western margin of the Shan Plateau extending up to about 1500 km from the Gulf of Mantaban through Mogok to eastern Himalayan Syntaxis (Mitchell et al., 2007; Searle et al., 2007). This belt consists of schist, gneiss, quartzite, marble, calc-silicate rock, locally granulite and migmatite with various granitoid intrusions. These metamorphic rocks were regionally metamorphosed under medium- to high-grade amphibolite facies and locally granulite facies conditions (e.g., Barley et al., 2003; Mitchell et al., 2007; Searle et al., 2007; Yonemura et al., 2013; Ye Kyaw Thu et al., 2016; 2017).

The Mogok-Kyatpyin area is located 200 km north of the Mandalay region and corresponds to the middle segment of the Mogok metamorphic belt. The study area is dominated by various types of high-grade gneiss associated with marbles and calc-silicate rocks (Fig. 1). These metacarbonate rocks were mainly intruded by various types of granitoid rocks including leucogranite, syenitic rocks, pegmatite and biotite microgranite.

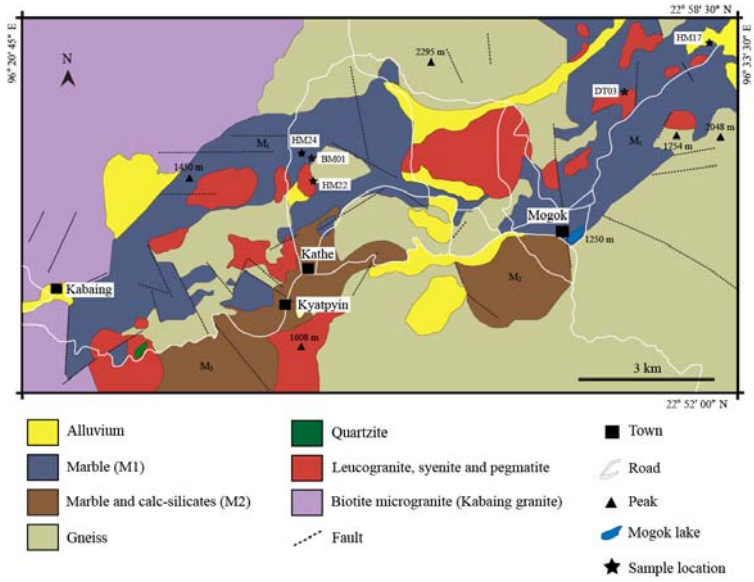

Figure (1). Geological map of the Mogok-Kyatpyin area (simplified from geological maps of Kyaw Thu, 2007; and Themelis, 2008).

Gneisses are widely distributed in the study area and occur as large block or thick bedded. The main exposures are garnet-biotite gneiss with local occurrence of garnet-sillimanite gneiss, garnet-pyroxene gneiss and garnet-cordierite gneiss. The collected

gneisses are medium to coarse-grained and show gneissose texture with alternating light and dark layers containing quartz, feldspar, biotite and garnet. Partial melting characters are also observed in some gneiss exposed at Hta-yan-sho mine and Nanpeit stream giving magmatic character. The common constituent minerals are quartz, feldspar, biotite and garnet with minor amount of zircon, graphite and ilmenite. Mineral abbreviation used in text, figure and table are after Whitney and Evans (2010). Common mineral assemblages of studied gneiss samples are shown in table 1.

Table (1). Mineral assemblages of the garnet-pyroxene gneiss and associated gneiss from the Mogok-Kyatpyin area.

Sample	Grt	Bt	Sil	Kfs	Qz	Pl	Crd	Opx	Rt	Ilm	Others
Garnet-pyroxene gneiss											
HM22	+	b		+	b	+	+	+		+	Zrn
Garnet-cordierite gneiss											
HM24	+	b		+	b	+	+			+	Zrn
BM01	+	b	i	+	b	+	+			+	Zrn, Gr
Garnet-sillimanite gneiss											
HM17	+	b	+	+	b	+			+	+	Zrn, Gr
Garnet-biotite gneiss											
DT03	+	b		+	b	+				+	Gr

+, present in matrix; i, inclusion in garnet; b, present both in matrix and as inclusion in garnet.

Petrography of observed gneiss samples

Garnet-orthopyroxene-cordierite gneiss (HM22 sample)

Garnet-orthopyroxene-cordierite gneiss is exposed at latitude 22° 55′ 27″ N and longitude 96° 25′ 07″ E. This gneiss is cropped out as blocks and occurs as alternating bands of felsic and mafic layers. The mineral assemblages are characterized by garnet, orthopyroxene, biotite, K-feldspar, plagioclase, and quartz with minor amount of Zrn and Ilm. The garnet-orthopyroxene-cordierite gneiss sample (HM22) consists roughly of medium- to coarse-grained garnet (~ 5%), orthopyroxene (10%), cordierite (5 – 10%), K-feldspar (15 – 20%), plagioclase (~ 15%), quartz (15 – 20%), biotite (15 – 20%), and other accessory minerals (~ 5%) of the visually estimated modal amount.

Garnet grains occur as subhedral to anhedral porphyroblasts and have an average size of 1 mm in diameter (Fig. 2a). Fine-grained quartz and biotite grains occur as inclusions. Some garnet grains are partially replaced by biotite around the rim. Orthopyroxene grains occur as subhedral to anhedral form and range in size from 0.5 – 0.7 mm in diameter (Figs. 2b and d). They commonly coexist with common matrix assemblages of garnet, cordierite, plagioclase, K-feldspar, quartz and biotite. Cordierite grains are observed as matrix phase and

range in size from 0.5 – 1 mm in diameter. The grain surface is dusty and commonly contains symplectitic grains of quartz and biotite (Figs. 2b and c). Biotite grains show brown to reddish brown color (Fig. 2), which is characteristic feature of high-grade metamorphism. They occur as isolated grains in matrix, aggregates around garnet and symplectitic phase with quartz in cordierite (Figs. 2b and c). Plagioclase and K-feldspar occur as common matrix grains (Fig. 2). Some K-feldspar grains are intergrown with plagioclase. Quartz is the most abundant mineral and occurs as subhderal to anhedral grains. It commonly occurs as subrounded inclusion grains in garnet (Fig. 2a) and also forms symplectitic grains with cordierite (Figs. 2b and c). Ilmenite occurs as accessory phase and forms elongated or subheral form. It also occurs as intergrowing phase with biotite. Elliptical or rounded zircon (Fig. 2d) occurs as minor phase in matrix.

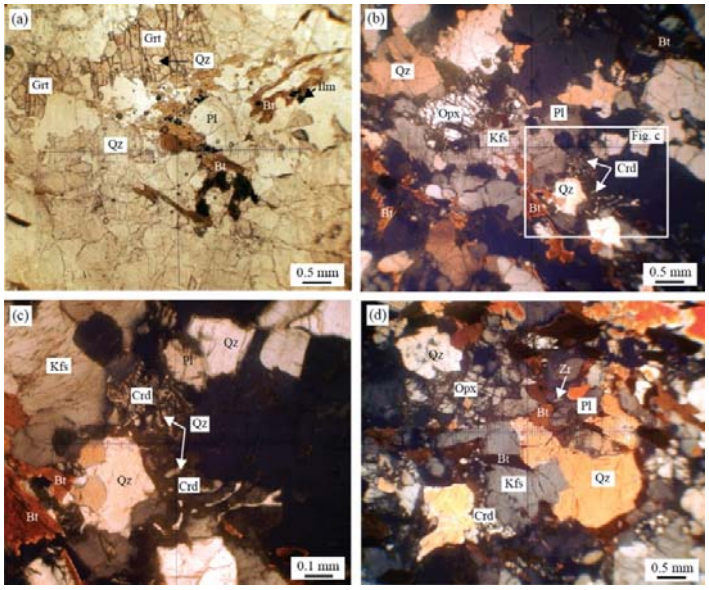

Figure (2). Photomicrograph of garnet-orthopyroxene-cordierite gneiss (HM22 sample) showing (a) anhedral garnet grain and surrounding matrix, (b) subhedral orthopyroxene grain in matrix coexisting with other primary phases, (c) enlarged view of the anhedral cordierite grain intergrown with quartz, and (d) subhedral orthopryoxene grains associated with biotite, quartz and plagioclase. All photomicrographs are under cross-polarized light except image (a), which is under plane-polarized light.

Garnet-cordierite gneiss (HM24 and BM01 samples)

Garnet-cordierite gneiss (HM24 and BM01 samples) are collected from latitude 22° 55′ 58″ N and longitude 96° 25′ 04″ E and latitude 22° 55′ 55″ N and longitude 96° 25′ 05″ E, respectively. The gneiss exposures occur as a block and mostly weathered. The mineral assemblages are characterized by garnet, cordierite, biotite, K-feldspar, plagioclase and quartz with minor amount of Zrn and Ilm. The garnet-cordierite gneisses (HM24 and BM01 samples) consist roughly of garnet (15 – 20%), cordierite (10 – 15%), K-feldspar and plagioclase (15 – 20%), quartz (15 – 25%), biotite (15 – 20%), and other accessory minerals (5%) of the visually estimated modal amount.

Garnet grains occur as subhedral to subrounded porphyroblasts coexisting with cordierite, K-feldspar, plagioclase, quartz and biotite (Fig. 3). The size ranges from 1 – 2 mm in HM24 sample (Fig. 3a), and 2 – 4 mm in BM01 sample (Fig. 3c). Sillimanite, quartz and

biotite grains commonly occur as inclusions in garnet (Figs. 3a, c and d). Some garnet grains are replaced by biotite along cracks and around the rim in HM24 sample (Fig. 3a). Cordierite grains occur as matrix phase (Fig. 3c) and around the garnet rim (Figs. 3a, c and d). They range in size from 0.2 – 0.5 mm in diameter. The grain surface is dusty and are commonly intergrown with quartz in HM24 sample (Fig. 3b) and intergrown with biotite and ilmenite in BM01 sample (Fig. 3d). Biotite grains show brown to reddish brown color, and occur as isolated grains (Fig. 3), aggregates across and around garnet grains (Fig. 3a) and symplectitic phase with ilmenite in cordierite (Fig. 3d). Plagioclase and K-feldspar occur as common matrix grains. Quartz grains occur as subhderal to anhedral grains in matrix and as a subrounded inclusion grains in garnets and as symplectitic grains with cordierite (Figs. 3.5b and c). In BM01 sample, Acicular or prismatic sillimanite grains occur as inclusions, and are rare in matrix (Fig. 3c). Ilmenite, zircon and graphite occur as accessory phase.

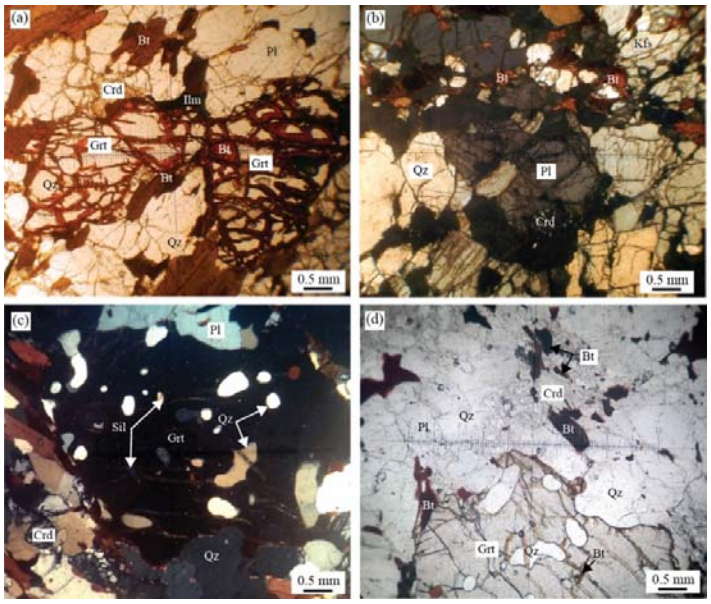

Figure (3). Photomicrograph of garnet-cordierite gneisses (HM24 and BM01 samples) showing (a) anhedral garnet porphyroblast replaced by secondary biotite aggregates along cracks and grain boundaries and (b) cordierite intergrown with quartz and surrounding matrix phases, (c) the garnet porphyroblast with sillimanite, biotite and quartz inclusions, and (d) symplectitic texture of anhedral cordierite with biotite and/or illmenite. All photomicrographs are under cross-polarized light except images (a) and (d) which are under plane-polarized light.

Garnet-sillimanite gneiss and garnet-biotite gneiss (HM17 and DT03 samples)

Garnet-sillimanite gneiss and garnet-biotite gneiss (HM17 and DT03 samples) are collected from latitude 22° 57′ 38″ N and longitude 96° 32′ 25″ E and 22° 56′ 58″ N and 96° 31′ 35″ E, respectively. The gneiss exposures are medium to thick bedded and the garnet-biotite exposures are mostly highly weathered. The mineral assemblages are characterized by garnet, sillimanite, biotite, K-feldspar, plagioclase and quartz with minor amount of Zrn, Ilm and graphite. The average composition of garnet-sillimanite gneiss and garnet-biotite gneiss (HM17 and DT03 samples) consists of garnet (15 – 25%), K-feldspar and plagioclase (20 – 30%), quartz (15 – 25%), biotite (20 – 25%), and other accessory minerals (5%) of the visually estimated modal amount.

Garnet grains occur as subhedral to anhedral porphyroblasts grains, and ranges in size from 1 – 3 mm in diameter (Figs. 4a, b and c). Quartz and biotite grains with an average size of 0.3 mm occur as inclusions in garnet (Figs. 4a, b and c). Some garnet grains are replaced by biotite along cracks in HM17 sample. Acicular or elongated sillimanite grains with an average size of 0.2 mm in diameter occur in matrix coexisting with garnet, biotite, plagioclase, K-feldspar and quartz (Fig. 4a). Biotite grains also show brown to reddish brown color, and occur as isolated grains (Figs. 4a, c and d), aggregates across and around garnet (Fig. 4a). Plagioclase and K-feldspar occur as common matrix grains (Fig. 4). Quartz grains occur as subhderal to anhedral grains in matrix and as a subrounded inclusion grains in garnets. Prismatic rutile grains occur in matrix (HM17 sample) coexisting with primary phases (Fig. 4b). Ilmenite, zircon and graphite occur as accessory phases.

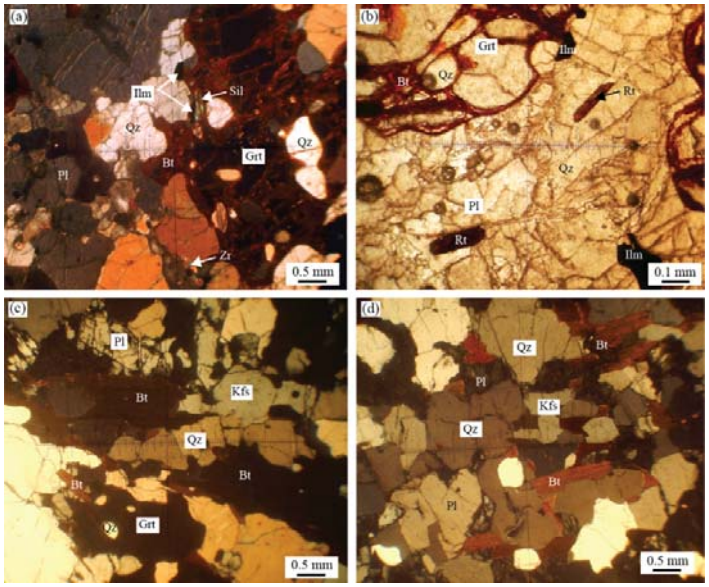

Figure (4). Photomicrograph of garnet-sillimanite gneiss and garnet-biotite gneiss (HM17 and DT03 samples) showing (a) the textural relationship of the garnet grains coexisting with sillimanite, biotite, quartz and plagioclase, (b) enlarged view of elongated rutile grains in the matrix, (c) the anhedral garnet porphyroblast and surrounding matrix, and (d) the primary matrix assemblage of garnet-biotite gneiss. All photomicrographs are under cross-polarized light except image (b), which is under plane-polarized light.

Discussion

Mineral reaction and petrogenetic grid in the KFMASH system

The figure (5) shows the pressure and temperature diagram (*P*–*T*) in the K_2O-FeO-MgO-Al_2O_3-SiO_2-H_2O (KFMASH) system for the metapelites of all bulk compositions (White et al., 2001). The high-grade assemblages of gneiss samples are characterized by Grt + Opx + Crd + Kfs + Pl + Bt + Qz + Ilm in HM22 sample, Grt + Crd + Kfs + Pl + Bt + Qz + Ilm in HM24 and BM01 samples, and Grt + Sil + Kfs + Pl + Bt + Qz + Rt + Ilm in HM17 sample. In HM22 sample, the peak assemblage may have formed through a partial melting reaction in the KFMASH system (Fig. 5) as follows:

Grt + Bt + Qz = Crd + Opx + Kfs + Liq (1)
Grt + Bt + Qz + Pl = Opx + Kfs + Liq (2)

However, the textural relation of garnet-orthopyroxene gneiss is complex and orthopyroxene crystals are closely associated with biotite, quartz and plagioclase (Figs. 2b and d). For normal metapelitic rocks biotite was also involved as a reactant in the following reactions:

Bt + Qz + Pl = Opx + Liq (+ Ilm) (3)
Qz + Bt + Pl = Grt + Opx + Kfs + melt (4)
Bt + Qz = Opx + Kfs + melt (5)

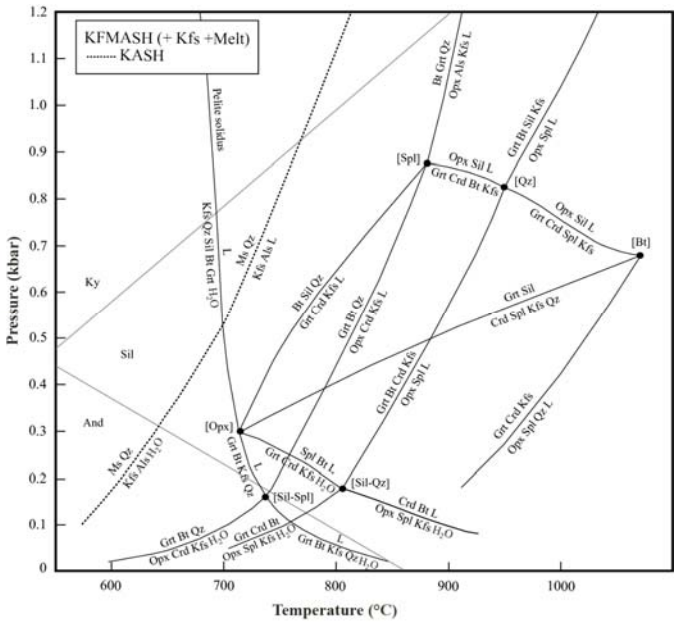

Figure (5). Pressure and temperature (*P–T*) diagram showing the mineral reactions in the K_2O-FeO-MgO-Al_2O_3-SiO_2-H_2O (KFMASH) system for the metapelites of all bulk compositions (after White et al., 2001).

For orthopyroxene-bearing sample (HM22), garnet grains are rarely observed as a reactant phase while biotite, quartz and plagioclase are often observed in association with orthopyroxene grains and this textural relationship indicates that garnet-absent reaction probably produces these orthopyroxene-bearing assemblages or garnet may be consumed according to garnet-bearing reactions.

In cordierite-bearing samples, several melt-related reactions were proposed to explain formation of cordierite under the high-grade amphibolite and granulite facies conditions. In garnet-cordierite gneiss, the formation of cordierite can be attributed by the following reactions:

Grt + Sil + Qz = Crd (6)
Bt + Sil + Qtz (+ Pl) = Crd + Kfs + melt (+ Ilm) (7)

Garnet grains contain acicular sillimanite and quartz inclusions (Figs. 3c and d), and anhedral cordierite grains form around garnet porphyroblasts (Figs. 3a, c and d). Therefore, the reactions (6) and (7) probably produce the cordierite formation. The symplectitic formation of cordierite–quartz (Figs. 2b, c and Fig. 3b) or cordierite-biotite symplectite (Fig. 3d) in the matrix of cordierite-bearing samples (BM01 and HM22) may be described by the reaction (8).

Grt + Melt = Crd + Bt + Qz (8)

In sillimanite-bearing gneiss sample and garnet-biotite gneiss sample, the formation of the peak assemblages may be attributed by the following reaction:

Grt + Melt (+ Ilm) = Bt + Sil + Qtz + Pl (9)

As shown in figure (5), although spinel and cordierite assemblages are not observed in the studied samples, the H_2O content in the cordierite structure can increase the stability field of cordierite toward the higher and lower pressure side.

Pressure and temperature (*P–T*) conditions and trajectory for the orthopyroxene-bearing and cordierite-bearing samples

The figure (6) shows pressure and temperature diagram in the K_2O-FeO-MgO-Al_2O_3-SiO_2-H_2O (KFMASH) system for the metapelites of all bulk compositions (White et al., 2001) combining with the X_{Fe} [=Fe/(Fe + Mg)] isopleth of garnet composition. The X_{Fe} [=Fe/(Fe + Mg)] was calculated using the composition of garnet from Mogok area (Yonemura et al., 2013) and that of garnet from Onzon area (Ye Kyaw Thu et al., 2017). The average pressure and temperature (*P–T*) estimations for the peak assemblages of garnet-orthopyroxene-cordierite gneiss (HM22 sample) and garnet-cordierite gneiss (HM24 and BM01 samples) display 6.8 kbar/850 ± 10 °C and 7 kbar/830 ± 20°C for the peak stage, respectively (Fig. 6).

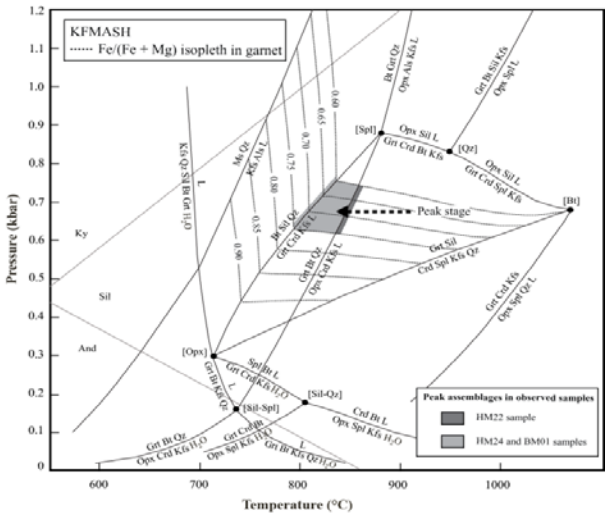

Figure (6). Pressure and temperature (*P–T*) diagram showing the mineral reactions in the K_2O-FeO-MgO-Al_2O_3-SiO_2-H_2O (KFMASH) system for the metapelites of all bulk compositions (after White et al., 2001) combining with the X_{Fe} [=Fe/(Fe + Mg)] isopleth of garnet composition employing the composition of garnet from Mogok area (Yonemura et al., 2013) and Onzon areas (Ye Kyaw Thu et al., 2017). Dashed arrows indicate the peak assemblages of garnet-orthopyroxene-cordierite gneiss (HM22 sample) and garnet-cordierite gneiss (HM24 and BM01 samples).

High-temperature estimation of 6.5–8.7 kbar/800–950 °C was reported from the same area for the garnet-orthopyroxene granulite. Based on the thermobarometric constraints, peak condition of 780–860 °C at 6.0–8.4 kbar was reported for spinel-bearing paragneiss,

cordierite-bearing paragneiss and associated garnet-biotite paragneiss from Onzon area, which is about 50 km southwest of the sampling area (Ye Kyaw Thu et al., 2016, 2017). The metamorphic conditions of the present study are consistent with the previously published estimations, and suggest the wide distribution of upper-amphibolite to granulite facies conditions in the middle segment of the Mogok metamorphic belt.

Based on the peak equilibrium conditions and textural relations, pressure and temperature trajectory was estimated for the orthopyroxene-bearing sample and cordierite-bearing samples (Fig. 7). In cordierite-bearing sample, fibrolitic sillimanite, quartz and biotite grains occur as relic inclusion in garnet, and probably joined the prograde path. Although spinel-cordierite assemblages are rare in the samples, it was reported from the cordierite-bearing paragneiss from Onzon area in which anhedral cordierite around garnet with higher X_{Mg} values than peak cordierite grains in matrix yield re-equilibration *P–T* conditions of about 4.0 kbar/620 °C (Ye Kyaw Thu et al., 2017). The middle segment was experienced similar metamorphic conditions and, therefore, the retrograde path was estimated based on the report of Onzon area and mineral relations.

They also proposed that the symplectitic cordierite grains probably formed during the early stage of exhumation under upper-amphibolite or granulite facies conditions around 0.8GPa/800 °C. Such re-equilibration during exhumation was also reported symplectitic aggregates of garnet + biotite + plagioclase + quartz in paragneisses with equilibrium conditions of 3.0–5.0 kbar/600–680 °C from the Sagaing ridge (Maw Maw Win et al., 2016; Enami et al., 2017). They interpreted that the formation of symplectite was related to fluid activity at late Oligocene based on monazite age in the paragneiss. Based on these facts, extensive re-equilibration likely occurred throughout the middle segment of the Mogok metamorphic belt at that time.

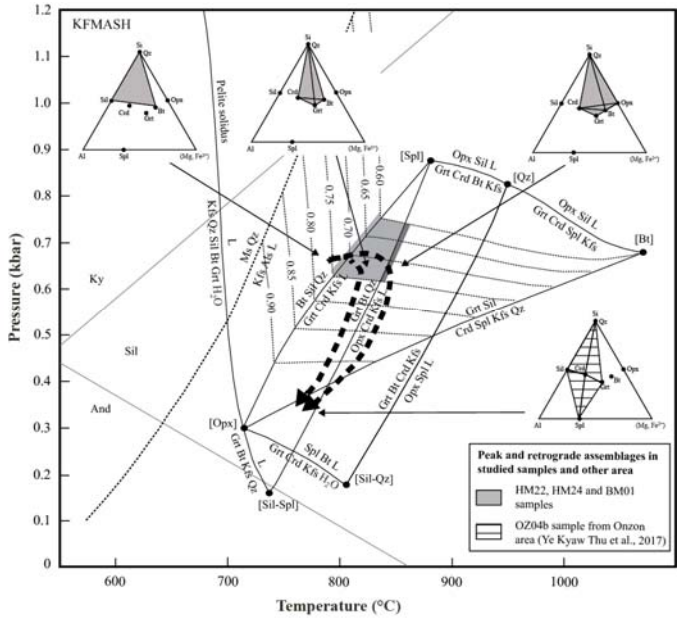

Figure (7). Pressure and temperature (*P–T*) diagram in the K_2O-FeO-MgO-Al_2O_3-SiO_2-H_2O (KFMASH) system for the metapelites of all bulk compositions (after White et al., 2001). Triangles in the FeO-MgO-Al_2O_3-SiO_2 system are also included showing the stability of mineral assemblages. Dashed arrows indicate the probable cooling paths for studied samples.

Conclusions

The Cenozoic Mogok metamorphic belt, extending for about 1500 km, lies at the western margin of the Shan-Thai Block, and forms a prominent part for understanding the continental evolution of Southeast Asia. The Mogok-Kyatpyin area occupies in the middle segment of the Mogok metamorphic belt. The high-grade assemblages of gneiss samples are characterized by Grt + Opx + Crd + Kfs + Pl + Bt + Qz + Ilm in HM22 sample, Grt + Crd + Kfs + Pl + Bt + Qz + Ilm in HM24 and with sillimanite inclusion BM01 samples, Grt + Sil + Kfs + Pl + Bt + Qz + Rt + Ilm in HM17 sample, and Grt + Kfs + Pl + Bt + Qz + Ilm in DT03 sample.

In the KFMASH system for the metapelites of all bulk compositions, the average pressure and temperature ($P - T$) conditions of garnet-orthopyroxene-cordierite gneiss sample and garnet-cordierite gneiss samples suggest 6.8–7 kbar/830–850 °C for the peak stage. The metamorphic conditions of the present study are consistent with the previously published estimations, and combining with other high-grade areas suggest the widespread distribution of upper amphibolite to granulite facies metamorphic rocks in the middle segment of the Mogok belt.

Based on the formation of symplectitic cordierite grains, re-equilibration probably formed during the early stage of exhumation under upper-amphibolite or granulite facies conditions. Such recrystallization combining with other reported high-grade areas likely occurred throughout the middle segment of the Mogok metamorphic belt at late Oligocene.

References

Barley, M.E., Pickard, A.L., Khin Zaw, Rak, P. and Doyle, M.G., 2003. Jurassic to Miocene magmatism and metamorphism in the Mogok metamorphic belt and the India-Eurasia collision in Myanmar. Tectonics, 22, doi.10.1029/2002TC001398.

Bertrand, G., Rangin, C., Maluski, H. and Bellon, H., 2001. Diachronous cooling along the Mogok metamorphic belt (Shan Scarp, Myanmar); the trace of the northward migration of the Indian syntaxis. Journal of Asian Earth Sciences, 19, 649-659.

Bertrand, G., Rangin, C., Maluski, H., Tin Aung Han, Ohn Myint, Win Maw and San Lwin, 1999. Cenozoic metamorphism along the Shan Scarp (Myanmar); evidences for ductile shear along the Sagaing Fault or the northward migration of the eastern Himalayan syntaxis? Geophysical Research Letters, 26, 915-918.

Bunopas, P., 1982. Paleogeographic History of Western Thailand and Adjacent Parts of South-east Asia: A Plate Tectonics Interpretation. pp. 810. Department of Mineral Resources, Thailand.

Enami, M., Nagaya, T. and Maw Maw Win., 2017. An integrated EPMA-EBSD study of metamorphic histories recorded in garnet. American Mineralogist, doi: 10.2138/am-2017-5666.

Kyaw Thu, 2007. The Igneous Rocks of the Mogok Stone Tract: Their Distribution, Petrography, Petrochemistry, Sequence, Geochronology and Economic Geology, PhD Dissertation, Yangon University.

Maw Maw Win, Enami, M. and Kato, T., 2016. Metamorphic conditions and CHIME monazite ages of Late Eocene to Late Oligocene high-temperature Mogok metamorphic rocks in central Myanmar. Journal of Asian Earth Sciences, *117*, 304-316.

Metcalfe, I. 1994. Gondwanaland origin, dispersion, and accretion of East and Southeast Asian continental terranes. Journal of South American Earth Sciences, 7, 333-347.

Metcalfe, I., 2013. Gondwana dispersion and Asian accretion: Tectonic and palaeogeographic evolution of eastern Tethys. Journal of Asian Earth Sciences, 66, 1-33.

Mitchell, A.H.G., Myint Thein Htay, Htun, K.M., Myint Naing Win, Thura Oo and Tin Hlaing, 2007. Rock relationships in the Mogok metamorphic belt, Tatkon to Mandalay, central Myanmar. Journal of Asian Earth Sciences, 29, 891-910.

Searle, M.P., Noble, S.R., Cottle, J.M., Waters, D.J., Mitchell, A.H.G., Tin Hlaing and Horstwood, M.S.A., 2007. Tectonic evolution of the Mogok metamorphic belt, Burma (Myanmar) constrained by U-T-/Pb dating of metamorphic and magmatic rocks. Tectonics, 26, TC3014.

Themelis T., 2008. Gems & mines of Mogok. A & T, Bangkok.

White, R.W., Powell, R., and Holland, T.J.B., 2001. Calculation of partial melting equilibria in the system Na_2O–CaO–FeO–MgO–Al_2O_3–SiO_2–H_2O (NCKFMASH). Journal of Metamorphic Geology. 19, 139–153.

Whitney, D.L. and Evans, B.W., 2010. Abbreviations for names of rock–forming minerals. American Mineralogist, 95, 185-187.

Ye Kyaw Thu, Enami, M., Kato, T. and Tsuboi, M., 2017. Granulite facies paragneisses from the middle segment of the Mogok metamorphic belt, central Myanmar. Journal of Mineralogical and Petrological Sciences, 112, 1–19.

Ye Kyaw Thu, Maw Maw Win, Enami, M. and Tsuboi, M., 2016. Ti-rich biotite in spinel and quartz-bearing paragneiss and related rocks from the Mogok metamorphic belt, central Myanmar. Journal of Mineralogical and Petrological Sciences, 111, 270–282.

Yonemura, K., Osanai, Y., Nakano, N., Adachi, T., Charusiri, P. and Tun Naing Zaw, 2013. EPMA U-Th-Pb monazite dating of metamorphic rocks from the Mogok Metamorphic Belt, central Myanmar. Journal of Mineralogical and Petrological Sciences, 108, 184-188.